

## Accepted Manuscript

Characterisation of kaolinite colloidal and flow behaviour using its crystallinity measurements

Bulelwa Ndlovu, Saeed Farrokhpay, Elizaveta Forbes, Dee Bradshaw

PII: S0032-5910(14)00817-1  
DOI: doi: [10.1016/j.powtec.2014.09.029](https://doi.org/10.1016/j.powtec.2014.09.029)  
Reference: PTEC 10548

To appear in: *Powder Technology*

Received date: 11 June 2014  
Revised date: 8 September 2014  
Accepted date: 11 September 2014



Please cite this article as: Bulelwa Ndlovu, Saeed Farrokhpay, Elizaveta Forbes, Dee Bradshaw, Characterisation of kaolinite colloidal and flow behaviour using its crystallinity measurements, *Powder Technology* (2014), doi: [10.1016/j.powtec.2014.09.029](https://doi.org/10.1016/j.powtec.2014.09.029)

This is a PDF file of an unedited manuscript that has been accepted for publication. As a service to our customers we are providing this early version of the manuscript. The manuscript will undergo copyediting, typesetting, and review of the resulting proof before it is published in its final form. Please note that during the production process errors may be discovered which could affect the content, and all legal disclaimers that apply to the journal pertain.

## Characterisation of kaolinite colloidal and flow behaviour using its crystallinity measurements

**Bulelwa Ndlovu<sup>1</sup>, Saeed Farrokhpay<sup>1\*</sup>, Elizaveta Forbes<sup>2</sup> and Dee Bradshaw<sup>1</sup>**

<sup>1</sup> *Julius Kruttschnitt Mineral Research Centre, 40 Isles Road, Indooroopilly, 4068, QLD, University of Queensland, Australia.*

<sup>2</sup> *CSIRO Process Science and Engineering, Bayview Avenue, Clayton, 3168, Victoria, Australia*

---

Corresponding author: S Farrokhpay

40 Isles Road, Indooroopilly, 4068, QLD, Australia.

email: s.farrokhpay@uq.edu.au

## Abstract

This study evaluates the possibility of predicting colloidal and flow behaviour of kaolinite suspensions by measuring kaolinite crystallinity. The Hinckley index of different samples was calculated from XRD spectra as an indicator of the crystallinity. Kaolinite samples with a high Hinckley index showed a defined platy morphology with smooth surfaces of low surface area, while progressively roughened basal planes with prevalent broken edges were observed in kaolinite samples of lower Hinckley indices. Despite similarity in the elemental composition, the kaolinite samples present different surface charge properties, likely due to variations in exposed pH dependent edge sites. Poorly crystallised kaolinite samples were characterised by higher yield stresses and viscosities. This study highlights the importance of crystallinity characterisation towards predicting colloidal behaviour and flow characteristics of kaolinite suspensions.

**Keywords:** kaolinite; Hinckley index; rheology; crystallinity; Snobrite; Q38, KGa2

## 1. Introduction

The ideal structure of kaolinite ( $\text{Al}_4(\text{Si}_4\text{O}_{10})(\text{OH})_8$ ) is composed of an octahedral sheet of gibbsite ( $\text{Al}(\text{OH})_3$ ) linked to a tetrahedral sheet of silica. Upon breakage, two different surfaces are formed. The basal plane-face results from the cleavage of one layer from another, while the edges arise due to the rupture of the ionic or covalent bonds within the layers. Therefore, kaolinite pseudo-hexagonal platelets are composed of two distinctly different planes, each with different charge properties. The edges are believed to carry a pH dependent charge determined by the protonation and deprotonation of exposed aluminol and silanol amphoteric groups [1, 2]. The charge on the edge sites characteristically changes from positive to negative with increasing pH. At the edge, point of zero charge (p.z.c), the charge on the edge site changes from positive to negative. The charge on the faces, however, is assumed to be largely due to the isomorphous substitution of higher valence ions with ions of a lower valence (e.g.  $\text{Si}^{4+}$  substitution by  $\text{Al}^{3+}$ ), resulting in a permanent negative charge [3]. However, a charge dependency of this site has also been proposed, not inconsistent with the hydrolysis of silicon in the surface plane [4].

There have been extensive studies on the physico-chemical properties of kaolinite including the effect of factors such as pH, electrolyte type and ionic concentration [5-7]. The importance of physical properties such as particle shape, aspect ratio and surface area towards suspension colloidal behaviour has also been demonstrated [4, 8-10]. However, little

consideration has been made to variations in kaolinite crystallinity and its importance in predicting kaolinite suspension rheology and colloidal behaviour.

The non-homogeneity of kaolinite in deposits from the same geographic locations has been acknowledged by many researchers. However, most variations have often been attributed to macroscopic deviations, principally in texture, hardness, mineral and chemical impurities. The differences in the sharpness and resolution of kaolinite X-ray peaks highlighted that kaolinite minerals can also present variations in crystallinity. A number of empirical relationships have since been developed for the estimation of the degree of crystallinity. The most widely used relation for kaolin minerals is that proposed by Hinckley [11] which uses peaks within a shorter angular range to facilitate optimal peak resolution and intensity for more accurate index calculation. This calculation yields a dimensionless number which normally varies between 0.2 to 1.5, where a higher index value is indicative of well crystallised kaolinite particles with a smooth surface structure and defined edges and basal planes [12]. However, this ordered morphology is altered in poorly crystallised particles with low Hinckley indices which then comprise a rough surface structure with ragged, broken edges across the basal surface.

The aggregation of kaolinite particles can occur in three main modes of association, namely face-face (FF), edge-face (EF) and edge-edge (EE). FF association leads to the formation of lamellar structured aggregates of low apparent volume per plate. This type of particle association is characterised by low suspension yield stresses. EF and EE associations, on the other hand, lead to three dimensional “house of cards” structures where the volume occupied or swept out by an individual particle is maximized, and the apparent volume fraction of the suspension is also a maximum. This results in more rheologically complex suspensions than would occur with FF association [2, 13]. The realignment from one form of particle association to another has traditionally been attributed to electrostatic attractive and repulsive forces between the edges and faces. It is generally believed that at pH values below the edge p.z.c, EF structures will exist due to the attraction between positively charged edges and negatively charged faces. This type of aggregation is enhanced in kaolinite particles, which inherently have thicker edges than other phyllosilicates such as muscovite or smectite. This renders the edge charge more significant. The changes in particle alignment as a function of pH are discussed in more detail by several researchers [1, 2, 7].

Although these are the forms of aggregation that have traditionally been assumed for kaolinite particles, recent study [12] demonstrated that particle aggregation may be more complicated depending on the crystallinity. It was demonstrated that for poorly crystallised kaolinite samples, self-aggregation may occur due to the hydrogen bonding between exposed silanol and aluminol broken edges on the basal surfaces of adjacent particles. This then results in additional randomised EE and EF structures, which were seen to have higher settling rates and bed densities than well crystallised kaolinite samples [12]. The flow properties (rheology) of kaolinite suspensions are already complicated due to the formation of heterocoagulated structures. Therefore, additional self-aggregation will likely result in even more complex suspension rheology. Such aggregation is also likely enhanced by a high frequency of broken edges as expected in poorly crystallised kaolinite particles. This means that, keeping all things constant, structural formation may differ for kaolinite samples with different crystallinity resulting in variable rheological characteristics. Moreover, differences in surface morphology from smooth to ragged surfaces may result in different surfaces being exposed and kaolinite samples of different crystallinity are likely to present dissimilar surface charge characteristics.

This study investigates whether there is a relationship between kaolinite crystallinity and its suspension colloidal behaviour, defined as surface charge and rheological characteristics in this case. The findings could be beneficial towards ongoing studies to more accurately characterise clay minerals or the characterisation of clay minerals.

## **2. Material and experimental methods**

### *2.1 Materials*

Three kaolinite samples (Snobrite, Q38 and KGa2) were chosen for this study, based on their differences in crystallinity as reported previously [12]; although they may be also different in composition or size distribution which will be discussed. These kaolinite samples were supplied in powder form. Snobrite and Q38 were provided by Unimin Australia Limited and KGa2 was from a mine site in Warren County, Georgia (USA) and supplied by the Clay Mineral Society (USA).

The mineralogy was determined using X-Ray Diffraction (XRD). Samples were micronized in ethanol and dried overnight at 40°C prior to measurement. XRD spectra were obtained using a PANalytical X'Pert Pro MPD powder diffractometer (manufactured by PANalytical,

Netherlands), equipped with an XCellerator detector. Samples were run with fixed divergence and anti-scatter slits, using Co-K $\alpha$  radiation. PANalytical's HighScore Plus Software (v3.0d) was used for phase identification and quantification using the Rietveld refinement method. XRD quantification determined the abundances of each kaolinite sample with purities of 89%, 85% and 99% for Snobrite, Q38 and KGa2, respectively (Table 1). The impurities comprised mainly of quartz and illite. It has previously been shown that these minerals do not affect the suspension rheology [14, 15]. While the colloidal behaviour can still be assumed to be largely due to the bulk mineralogy i.e. kaolinite, the synergistic or antagonistic effects of these impurities on the colloidal properties is worth investigating in future analyses.

## 2.2 Sample characterisation

*Crystallinity measurements:* The crystallinity of each kaolinite sample was estimated using the Hinckley index calculation [16]. This is ratio of the sum of the net peak intensities of the  $1\bar{1}0$  and  $1\bar{1}1$  reflections measured from the inter-peak background to the total net peak intensity of the  $1\bar{1}0$  peak measured from the background of the whole X-ray diffraction record. The  $<2\ \mu\text{m}$  fraction of each kaolinite sample was also extracted to minimise the quartz material for Hinckley index calculation. Un-oriented samples were then analysed with the XRD spectra scanned over a  $2\Theta$  range of  $20\text{-}32^\circ$   $2\Theta$ , covering the spectra for relevant Hinckley peaks.

*Particle morphology:* A field emission, environmental FEI Quanta 400 (FEI, USA) scanning electron microscope (ESEM) was used to investigate the surface morphology of each kaolinite. Representative samples were suspended in isopropanol and sonicated for five minutes. A drop of each suspension was then placed on a polished carbon block and allowed to evaporate prior to examination.

*Particle size and surface area:* The particle size distribution of each kaolinite was estimated using wet size light scattering technology using a Malvern Mastersizer (Malvern, UK). In each case, 0.5 g samples were dispersed in water, and the pH adjusted to pH 10. At these conditions, kaolinite particles have high enough surface charge for repulsion which enhances dispersion. Sodium hexametaphosphate (Calgon) was also used as a dispersant at a concentration of 1 wt%. The sample was sonicated for 60 s at 50% ultrasonic power for 60 s before the measurement. Pump and stirring speeds of 330 rpm and 350 rpm respectively were used during the measurement. For each kaolinite, tests were carried out in triplicate for

reproducibility. The size distribution shown for each mineral is representative of the average size distribution of three individual measurements.

BET specific surface areas of each kaolinite were measured by a Micromeritics Tristar 3000 BET Surface Area Analyser (Micromeritics, USA) using N<sub>2</sub> adsorption at 200°C.

#### *Suspension colloidal characterisation*

*Zeta potential measurements:* Zeta potential measurements were performed using a ZetaProbe Analyzer (Colloidal Dynamics, USA). In each case, a 5 wt% suspension was prepared in 250 mL of 0.001M KCl solution. The pH was adjusted accordingly, using an automatic titration using solutions of 0.2M KOH and 0.2M HCl. The measurements were taken through a downward ramp from pH 11 to pH 3. The ZetaProbe Analyzer uses the electrophoretic mobility and Smoluchowski's equation to calculate the zeta potential at each pH condition. The pH at which the zeta potential is zero is the iso-electric point (i.e.p).

*Potentiometric titration measurements:* The point of zero charge (p.z.c.) of each kaolinite was determined using the Roberts-Mular potentiometric titration. This method works on a principle of ion exchange, with the pH measured at different ionic strengths of the solution [17]. Suspensions consisting of 1g representative samples of each mineral in 50 mL of 0.001M KCl were prepared, with each suspension adjusted to a different pH value (ranging from pH 3 to pH 11). The ionic strength of each solution was then raised from 0.001M to 0.1M by the addition of the appropriate amount of dry KCl crystals. The pH of the resulting solution was measured to give a final pH. The difference in the initial and final pH values ( $\Delta\text{pH}$ ) is plotted against the final pH. The pH value at which  $\Delta\text{pH}$  is zero indicates the point p.z.c of each kaolinite.

*Rheological characterisation:* Suspensions were prepared at varying solid concentrations (5 to 25 vol%). Each slurry sample (~50 cm<sup>3</sup>) was pre-sheared at a high shear rate of 300 s<sup>-1</sup>. Preliminary tests showed hysteresis loops when readings were taken at increasing and decreasing rates of shear. This was overcome by performing continuous ascendant and descendant shear viscosity runs until both could be represented by a common curve. At this point, the system was assumed to be shear equilibrated and dispersed. The stress - strain tests were then conducted in a shear rate controlling regime, within the range 0.1 s<sup>-1</sup> to 400 s<sup>-1</sup>, over 45 s. Tests were conducted using an Anton Paar DSR 300 rheometer, with a standard bob and cup geometry. The bob has a roughened surface to minimise slipping effects.

The resulting rheograms demonstrated pseudoplastic behaviour, as shown in Fig. 1. The Herschel Bulkley model was used to estimate the suspension yield stress and shear thinning index (Equation 1).

$$\text{Herschel Bulkley model:} \quad \tau = \tau_0 + \eta_p \dot{\gamma}^n \quad \text{Equation 1}$$

where  $\tau$  is the shear stress (Pa),  $\tau_0$  is the yield stress (Pa),  $n$  is the shear thinning factor,  $\eta_p$  is the viscosity (Pa.s) and  $\dot{\gamma}$  is the shear rate ( $s^{-1}$ ) [18].

### 3. Results and discussion

#### 3.1 Crystallinity measurements

As discussed above (section 2.2), the crystallinity of the kaolinite samples was determined using the Hinckley index. An index of 0.99 was calculated for Snobrite, suggesting that it is a well crystallised kaolinite. Q38 and KGa2, on the other hand, had lower indices of 0.80 and 0.30, respectively. On this basis the crystallinity decreased in the order Snobrite > Q38 > KGa2 in the agreement with the previously reported data [12]. As discussed earlier, the different kaolinite samples have different impurities comprised mainly of quartz and illite. Therefore, in order to remove the effect of quartz, Du et al. [12] have only analysed the <2  $\mu\text{m}$  fraction of their kaolinite samples. The Hinckley index for the <2 $\mu\text{m}$  fractions of Snobrite, Q38 and KGa2 were found to be 1.03, 0.80 and 0.30, respectively. The Hinckley indices for Snobrite and KGa2 (0.99 and 0.30, respectively) are close to those reported by Du et al (0.92 for Snobrite and 0.40 for KGa2), considering the different samples used in these two works, also the accuracy of the applied methodology in each work. The reported HI values for KGa2 were found in the range of 0.24 to 0.41 (with many around 0.32). In particular, Metz & Grano [19] have reported a range of  $0.37 \pm 0.05$  for KGa2 Hinckley index. However, the HI value found for Q38 (0.80) is much higher than the value of 0.49 reported by Du et al [12]. It should be remembered that Q38 is an industrial sample and it is not homogeneous. Therefore, the properties may vary from sample to sample. Moreover, the authors were not able to find any additional data for Q38 (other than that quoted by Du et al) for comparison. It should be mentioned that the rheological behaviour of Q38 suspensions in this study more closely resembles that of Snobrite suspensions rather than KGa2 suspensions. This behaviour is in agreement with the measured Hinckley index and crystallinity in this study, rather than that reported by Du et al. [12].



Fig. 2A shows the XRD spectra of the different kaolinite samples for both bulk sample and  $<2\ \mu\text{m}$  fraction. It can be seen that for Snobrite sample, quartz, calcite and dolomite are removed by the separation while the smectite content is enhanced. It should be mentioned that the presence of smectite in the samples was identified by first separating the  $<2\ \mu\text{m}$  size fraction of the samples and then Ca exchanging the  $<2\ \mu\text{m}$  fractions to accentuate the smectite peaks. All samples were progressively treated to ethylene glycol as they react differently. KGa2 is virtually unchanged and for Q38, the quartz and illite content has been reduced. An example of Hinckley index calculation is also provided in Fig. 2B. Table 1 shows also the characterisation of the bulk sample and  $<2\ \mu\text{m}$  size fraction of each sample.

### *3.2 Particle size and surface area characterisation*

The surface morphology of Snobrite, Q38 and KGa2 was investigated using scanning electron microscopy (SEM). A comparison of the samples used in this study is given in Fig. 3. The SEM images show that the three kaolinite samples have extensive kaolinite faces with different dimensions. Snobrite has relatively smooth basal planes. This kaolinite has defined euhedral platy morphology, with clear edges and basal planes. Q38 and KGa2 have a more complex basal surface structure, with the appearance of ragged, broken nano-sized edges across the areas of the basal surface. This structure differs from the typical euhedral to subhedral platy morphology of most kaolinites. The classic euhedral morphology is almost completely altered. Instead, the sample comprises nano-sized randomly oriented platelets, with no clear basal plane as is observed in Snobrite or Q38.

The SEM images are in agreement with the trend demonstrated by the calculated Hinckley indices, with Snobrite having the highest crystallinity and existing as smooth platelets. The appearance of broken edges on the basal faces results in the measured lower Hinckley index of Q38. KGa2 is poorly crystallised with the platy morphology almost completely destroyed. These trends are in agreement with previous reported results [12, 20, 21]. It should be also mentioned that, the crystal sizes in KGa2 are clearly smaller than the other two samples. This is an important factor as it can influence both crystallinity and BET surface area. It is also worth mentioning that the sizes quoted are based on Malvern measurements. This measurement equates the volume of a particle to that of a sphere of equivalent volume. Therefore, particle shape is not taken into consideration. In fact, the Malvern measurement becomes increasingly inaccurate with a larger deviation from sphericity as in platy or elongated particles. Therefore, while particle size differences are demonstrated in this study,

the surface area as measured by the BET analysis may provide a better indication of area and size differences between the kaolinites.

In order to estimate whether the differences due to crystallinity are reflected in particle size characterisation, the particle size distributions of all three kaolinites were estimated using conventional Malvern light scattering analysis. Fig. 4 shows that both Snobrite and Q38 have similar particle size distributions but coarser than KGa2. It is worth noting that there is a discrepancy between the particle sizes when estimated using SEM images and light scattering analysis (Fig. 3 and Fig. 4). Indeed, the primary particle sizes of the kaolinites by SEM are smaller than those measured using light scattering. However, light scattering analysis estimates the size of particles by equating their volume to that of a sphere of equivalent volume (equivalent sphere theory). This is misleading for irregular shaped particles, and the inaccuracy of this measurement becomes further exaggerated with a larger deviation from sphericity, as in the case of fibrous or platy particles (e.g. kaolinites). The proportion of <2  $\mu\text{m}$  component of the samples was further investigated using centrifuge. It was found that KGa2 sample consist more 96% of the <2  $\mu\text{m}$  fraction, while this figure for Snobrite and Q38 was between 60-65%. This further confirms the small crystal size for KGa2 sample. The amount of >63  $\mu\text{m}$  (sometime referred as “silt”) was found to be negligible for all samples. The particle size distribution of all three kaolinite samples can be better estimated using the  $d(0.1)$ ,  $d(0.5)$  and  $d(0.9)$  data presented in Table 2.

BET specific area measurements showed that Snobrite with the highest Hinckley index and particle size has the lowest surface area of 14.9  $\text{m}^2/\text{g}$  (Table 2). On the hand, KGa2, with the lowest Hinckley index, has the highest specific surface area of 20.3  $\text{m}^2/\text{g}$ . Q38 with an intermediate crystallinity index had a specific area of 19.2  $\text{m}^2/\text{g}$ . Therefore, the specific surface area increases as the particles become less crystalline. This is expected since there is a gradual transition from a platy structure in Snobrite to a more voluminous arrangement in KGa2.

### *3.3 Surface charge characterisation*

The surface charge properties of kaolinite have been studied extensively, with most studies using the zeta potential measurement as a sole means to characterise charge [3, 22, 23]. However, the application of this technique to kaolinite samples is compromised by its inherent assumption of spherical morphology and it has been acknowledged that extra precaution must be taken when analysing the charge properties of this group minerals [24,

25]. The inaccuracy of the zeta potential method for clay minerals has been demonstrated through the deviation of the i.e.p and the p.z.c. These values coincide for isotropically charged particles such as quartz, but differ for anisotropically charged particles [26, 27].

Ideally, correction of the zeta potential measurement and accurate estimation of the overall surface charge of kaolinite particles would require knowledge of the relative charge density and surface area of the different planes. Such information is most easily attained for particles with a smooth surface structure, but becomes increasingly difficult for poorly ordered structures [4]. In the absence of knowledge on the relative charges, the zeta potential measurement merely provides an average charge estimate, which can be misleading if viewed in isolation. Moreover, it is unclear what this average zeta potential measurement represents, since for anisotropically charged particles such as kaolinite, the i.e.p. (determined by the zeta measurement) does not correspond to the p.z.c. (determined by titration). Therefore, it cannot be indicative of a zero potential condition. The i.e.p. in this case may merely represent an apparent value, dependent only on the plane of measurement and with no physical implication. The p.z.c. however, is most likely a representation of the pH at which the positive charge on one plane, balances out the negative charge on another plane in a particle. The ambiguity around these parameters, for anisotropically charged minerals, requires their combined use for a comprehensive estimation of the degree of charge anisotropy. The Roberts Mular titration, from which the p.z.c. can be estimated, is based on a principle of ion exchange and is not subject to artefacts arising from particle morphology [17]. For this reason, the surface charge properties of the kaolinite samples were investigated using the zeta potential and Roberts Mular titration measurements.

A comparison of the zeta potential values for the three kaolinite samples (Fig. 5) shows a higher rate of change of the zeta potential for the poorly crystallised KGa2 than in well-crystallised Snobrite and Q38 throughout the pH range. This may be due to the high concentration of exposed hydroxyl groups on the basal faces, such that KGa2 is more sensitive to changes in pH. As a result an i.e.p at circa pH 3.8 was measured for KGa2. This is within the typically reported range for kaolinite i.e.p (pH 2.8 to 4.2) [28, 29]. No isoelectric points were detected for Snobrite and Q38 within the studied pH range.

Potentiometric titrations were conducted over the range pH 2 to pH 11. The results (Fig. 6) show a net p.z.c. at pH 3.9 for Snobrite, pH 3.1 for Q38, and pH 7.1 for KGa2. At these conditions, it is expected that there is an equal charge balance between the positively and

negatively charged planes. In each case, pH conditions below the p.z.c. represent the range in which the particle surface carries an overall positive charge, while conditions above the p.z.c. are representative of an overall negative particle surface charge.

A comparison of the i.e.p. and p.z.c. values for each kaolinite samples gives an indication of the degree of charge anisotropy, where a large deviancy between these values is indicative of a high degree of charge anisotropy (and a large deviation from isotropic behaviour). In each case i.e.p. is different from p.z.c.. This demonstrates that kaolinite samples do indeed differ from isotropically charged minerals. In the case of KGa2, however, a clear disparity is observed between the measured i.e.p. (pH 3.8) and p.z.c. (pH 7.1) indicating a high degree of charge anisotropy.

The observed differences in the i.e.p and p.z.c values across the three kaolinite samples demonstrate that crystallinity does indeed play a role in the measured values. It is important to note that the i.e.p. of the aluminol and silanol edge sites of kaolinite has been previously reported from pH 5 to pH 7 [30, 31], coinciding with the measured p.z.c. of KGa2 (pH 7.1). With a high frequency of exposed edge sites, it may be expected that the measured p.z.c. of KGa2 would be similar to that of the edges.

If the p.z.c. of KGa2 is indeed elevated due to the high frequency of edge sites on the surface, it is then expected that as particles become less crystalline, higher p.z.c values closer to the edge p.z.c (pH 5-7) are likely. With a predominantly platy structure, a p.z.c. value greater than Snobrite (pH 3.1), but less than KGa2 (pH 7.1) is expected for Q38. A p.z.c. within this range is observed for Q38 (pH 3.9). This then suggests that the edge i.e.p. may be, in part, dependent on the particle crystallinity, and will not always occur within the traditionally specified range. It is also worth noting, that the p.z.c. values of all the minerals are likely affected by the impurities present in each sample. This would be more evident in Snobrite and Q38, both with a lower degree of purity than KGa2. Here, it is more likely that the measured p.z.c. values are not only due to kaolinite, but also attributable to the illite and quartz contained in the samples. The p.z.c. values of these minerals have previously been measured at pH 2.3 for quartz and pH 6.8 for illite [15]. Therefore, any elevation in the p.z.c value due to edge sites could be depressed by these impurities, resulting in a lower measured value.

### 3.4 Rheological characterisation

The rheological characteristics of kaolinite and other clay minerals suspensions have been extensively studied [5, 8, 15]. In general, mineral slurry behaviour tends to shift from Newtonian to strongly non-Newtonian as the solid concentration increases [31].

Rheological tests were performed at pH 9 (adjusted using NaOH) as it is the pH at most unit operations (e.g. flotation). As previously stated, it is generally believed that at pH conditions below the edge i.e.p, EF structures exist due to the electrostatic attraction between positively charged edges and negative faces. Therefore, at pH conditions well above the edge i.e.p, the system should become dispersed, due to the repulsion between edge and basal face sites. On this basis, it is generally assumed that all kaolinite suspensions will predominantly comprise a combination of EE and dispersed structures at pH 9 [7]. Such suspensions would be characterised by low yield stresses and viscosities. However, as it has been demonstrated that crystallinity results in different surface charge properties, it is likely that differences in particle crystallinity will also lead to variations in rheological characteristics.

The differences in surface charge characteristics have suggested that the edge i.e.p value may be in part dependent on the particle crystallinity. If the p.z.c. does indeed represent the pH at which the charge differential between negatively and positively charged sites is maximum then strong EF structures would be expected at this condition. This may also represent the pH at which the positive charge on the edge is greatest, after which the magnitude of the positive charge decreases, becoming negative at some  $\text{pH} > \text{p.z.c}$ . Therefore, the edge p.z.c of Snobrite may occur at some  $\text{pH} > 3.1$ , Q38 at  $\text{pH} > 3.9$  and KGa2 at  $\text{pH} > 7.1$ . Although the exact edge p.z.c is unknown, it is less likely that the edge sites in Snobrite and Q38 will carry a positive charge at pH 9, as this occurs well away from the measured p.z.c values. However, there is a higher probability of positively charged or near positive edge sites in KGa2 particles, owing to the higher p.z.c. value (pH 7.1). If self-aggregation resulting from broken edges of poorly crystallised surfaces occurs as postulated by Du et al. [12], more complex suspension rheology will be observed for Snobrite and Q38 suspensions. Such aggregation is likely higher in poorly crystallised Q38 than Snobrite of high crystallinity, and will result in suspensions with a yield stress.

A comparison of the yield stresses of suspensions of each kaolinite at pH 9 is given in Fig. 7. The results show a characteristic increase in the yield stress with increasing solid concentration for all kaolinite samples. At concentrations less than 10 vol%, all kaolinite

suspensions are characterised by low yield stresses, after which a marked difference is observed between different kaolinite types. At equivalent concentrations, KGa2 suspensions are characterised by significantly higher yield stresses than Q38 samples, which in turn have higher yield stresses than Snobrite suspensions. This suggests that at pH 9, the degree of complexity in structural formation decreases in the order KGa2 > Q38 > Snobrite. This is in agreement with the predicted EE-EF formation in KGa2 suspensions relative to less complex dispersed EE structural formation in Snobrite and Q38 suspensions at pH 9. The nature of pseudoplastic flow behaviour is such that upon yielding, the structures formed will still resist deformation and sometimes flow does not even occur until destruction of the internal networks is completed [6]. The shear thinning index gives an indication of the degree of resistance to deformation, where a thinning index close to 1 more closely resembles a Bingham fluid where free flow is experienced upon yielding. However, lower indices are indicative of a greater resistance to flow, even after yielding. A greater resistance to flow is expected for complex structures with high yield stresses. Fig. 8 gives a comparison of the shear thinning indices of the kaolinite samples as a function of solid concentration.

All kaolinite samples show a gradual decrease in the shear thinning index, suggesting that the resistance to flow increases with solid concentration. This is expected due to the higher probability of aggregation in each case. However, at an equivalent concentration, KGa2 suspensions have lower shear thinning indices than Q38 suspensions which in turn has lower indices than Snobrite suspensions. This indicates that the resistance to flow is much higher in KGa2 than in Q38 or Snobrite, further suggesting the higher degree of complexity in structural formation of poorly crystallised KGa2.

It is also acknowledged that kaolinite samples may have some organic matter naturally which might affect their suspension rheological behaviour. However this was not investigated in the current study and it is suggested the presence of such material and its effect on the colloidal behaviour of kaolinite to be considered in future work.

#### **4. Conclusions**

The crystallinity of different kaolinite samples were studied using Hinckley index. Kaolinite samples of different crystallinity were found to present different surface charge properties and colloidal behaviour. The poorly crystallised kaolinite samples more closely represent the charge properties of exposed edge surfaces. The surface charge properties of well crystallised

kaolinite samples, on the other hand, more closely represent the charge properties of the extensive smooth basal planes (faces). Suspensions containing low crystallinity kaolinite samples present higher suspension yield stresses and viscosities than high crystallinity kaolinite samples which can impact the process behaviour of the kaolinite bearing suspensions.

It is concluded that early characterisation of kaolinite type could be beneficial towards better understanding and predicting their behaviour. It is acknowledged that a wider range of samples of kaolin differing in crystallinity may be needed to validate the results. As such samples are not easily available it is recommended to deliberately manipulate the crystallinity of kaolin, for example at high temperature or dry grinding, for future work.

### **Acknowledgments**

The financial support from CSIRO in form of a Flagship Collaboration Fund (Minerals Down Under) is acknowledged. Invaluable laboratory support in performing XRD analysis and spectral interpretation was provided by Dr. David Steele (JKTech) and Dr. Peter Self (CSIRO).

### **References**

- [1] P.F. Luckham S. Rossi: The colloidal and rheological properties of bentonite suspensions, *Adv. Colloid Interface Sci.*, 82 (1999) 43-92.
- [2] B. Rand I.E. Melton: Particle interactions in aqueous kaolinite suspensions: I. Effect of pH and electrolyte upon the mode of particle interaction in homoionic sodium kaolinite suspensions, *J. Colloid Interface Sci.*, 60 (1977) 308-320.
- [3] S.B. Johnson, A.S. Russell, P.J. Scales: Volume fraction effects in shear rheology and electroacoustic studies of concentrated alumina and kaolin suspensions, *Colloids Surf., A*, 141 (1998) 119-130.
- [4] P.J. Scales, F. Greiser, T.W. Healy: Electrokinetics of the muscovite mica - aqueous solution interface, *Langmuir*, 6 (1990) 582-589.
- [5] A.J. McFarlane, J. Addai-Mensah, K. Bremmell: Rheology of flocculated kaolinite dispersions, *Korea-Aust. Rheol. J.*, 17 (2005) 181-190.
- [6] H.A. Barnes, J.F. Hutton, K. Walters: *An Introduction to Rheology*, Rheology Series 3, Elsevier, Amsterdam, 1989.
- [7] S.B. Johnson, G.V. Franks, P.J. Scales, D.V. Boger, T.W. Healy: Surface chemistry-rheology relationships in concentrated mineral suspensions, *Int. J. Miner. Process.*, 58 (2000) 267-304.

- [8] H. Tateyama, P.J. Scales, M. Ooi, N. S., K. Rees, T.W. Healy: X-ray diffraction and rheology study of highly ordered clay platelet alignment in aqueous solutions of sodium tripolyphosphate, *Langmuir*, 13 (1997) 2440-2446.
- [9] R.G. de Krester, P. Scales, D.V. Boger: Surface chemistry-rheology inter relationships in clay suspensions, *Colloids Surf., A*, 137 (1998) 307-316.
- [10] S. Farrokhpay: The importance of rheology in mineral flotation: a review, *Miner. Eng.*, 36–38 (2012) 272–278.
- [11] D. Hinckley: Variability in “crystallinity” values among the kaolin deposits of the Coastal Plain of Georgia and South Carolina, *Clays Clay Miner.*, 11 (1963) 229-235.
- [12] J. Du, G.E. Morris, R.A. Pushkarova, R.S. Smart: Effect of surface structure of kaolinite on aggregation, settling rate, and bed density, *Langmuir*, 26 (2010) 13227-13235.
- [13] G. Lagaly: Colloid clay science, in F. Bergaya, B.K.G. Theng, G. Lagaly (Eds.), *Handbook of Clay Science*, Elsevier, Amsterdam, 2006, pp. 141-246.
- [14] B.N. Ndlovu, M. Becker, E. Forbes, D.A. Deglon, J.P. Franzidis: The influence of phyllosilicate mineralogy on the rheology of mineral slurries, *Miner. Eng.*, 24 (2011) 1314-1322.
- [15] B.N. Ndlovu, E. Forbes, S. Farrokhpay, M. Becker, D. Bradshaw, D.A. Deglon: A preliminary rheological classification of phyllosilicate group minerals, *Miner. Eng.*, 55 (2014) 190-200.
- [16] A. Plancon, R.F. Giese, R. Synder: The Hinckley index for kaolinites, *Clay Miner.*, 23 (1988) 249-260.
- [17] A.L. Mular R.B. Roberts: A Simplified method to determine isoelectric points of oxides, *Transactions of the Canadian Institute of Mining and Metallurgy*, 69 (1966) 438-439.
- [18] M. He E. Forssberg: Influence of slurry rheology on stirred media milling of quartzite, *Int. J. Miner. Process.*, 84 (2007) 240-251.
- [19] V. Metz J. Grano: Stirring effect on kaolinite dissolution rate, *Geochim. Cosmochim. Acta*, 65 (2001) 3475–3490.
- [20] M. Zbik, N.A. Raftery, R.S.C. Smart, R.L. Frost: Kaolinite platelet orientation for XRD and AFM applications, *Appl. Clay Sci.*, 50 (2010) 299-304.
- [21] M. Zbik R.S.C. Smart: Nanomorphology of kaolinites: comparative SEM and AFM studies, *Clay and Clay Minerals*, 46 (1998) 153-160.
- [22] G.E. Morris, D. Fornasiero, J. Ralston: Polymer depressants at the talc-water interface: adsorption isotherm, microflotation and electrokinetic studies, *Int. J. Miner. Process.*, 67 (2002) 211-227.
- [23] K.E. Bremmell J. Addai-Mensah: Interfacial chemistry mediated behaviour of colloidal talc dispersions, *J. Colloid Interface Sci.*, 283 (2005) 1173-1182.
- [24] J.D. Miller, J. Nalaskowski, B. Abdul, H. Du: Surface characteristics of kaolinite and other selected two layer silicate minerals, *Can. J. Chem. Eng.*, 85 (2007) 617-624.
- [25] W.N. Rowlands R.W. O'Brien: The dynamic mobility and dielectric response of kaolinite particles, *J. Colloid Interface Sci.*, 175 (1995) 190-200.



- [26] M. Subbanna, Pradip, S.G. Malghan: Shear yield stress of flocculated alumina–zirconia mixed suspensions: effect of solid loading, composition and particle size distribution, *Chem. Eng. Sci.*, 53 (1998) 3073-3079.
- [27] M. Alvarez-Silva, A. Uribe-Salas, M. Mirnezami, J.A. Finch: The point of zero charge of phyllosilicate minerals using the Mular–Roberts titration technique, *Miner. Eng.*, 23 (2010) 383-389.
- [28] F. Miu, Q. Zhao, L. Lui: Experimental study on the electrokinetics of kaolinite particles in aqueous suspension, *Physiochem. Probl. MI.*, 49 (2013) 659-672.
- [29] M.T. García-González, C. Vizcayni, J. Cortabitarte: Effect of kaolinite and sulfate on the formation of hydroxyl-aluminium compounds, *Clays Clay Miner.*, 48 (2000) 85-94.
- [30] R.S.C. Smart, M. Zbik, G.E. Morris: Crystallinity differences in kaolinite samples, in *Proceeding of the UBC-McGill Biennial International Symposium on Fundamentals of Mineral Processing*, Hamilton, Canadian Institute of Mining, Metallurgy and Petroleum, 2004, pp. 215-228.
- [31] E. Tombácz M. Szekeres: Surface charge heterogeneity of kaolinite in aqueous suspension in comparison with montmorillonite, *Appl. Clay Sci.*, 34 (2006) 105-124. .

## TABLES

Table 1 – XRD characterisation of Snobrite, Q38 and KGa2, bulk sample and <2  $\mu\text{m}$  fraction

Bulk sample (wt%)								
	kaolinite	quartz	calcite	dolomite	anatase	rutile	illite- mica	smectite
Snobrite	89	5	2	2	<1			2
KGa2	99	<1			1			
Q38	85	5			1	<1	9	
< 2 $\mu\text{m}$ size fraction (wt%)								
Snobrite	96	<1			<1			4
KGa2	99	<1			<1			
Q38	91	2			1		5	1

Table 2 – Characterisation of kaolinite samples

	d(0.1) ( $\mu\text{m}$ )	d(0.5) ( $\mu\text{m}$ )	d(0.9) ( $\mu\text{m}$ )	BET surface area ( $\text{m}^2/\text{g}$ )	Hinckley index
Snobrite	0.60	4.52	21.73	14.9	0.99
KGa2	0.54	4.91	16.28	20.3	0.30
Q38	0.56	4.39	17.24	19.2	0.80

### Figures Captions

Fig. 1 - Rheogram of the kaolinite suspensions at 15 vol% (pH 9)

Fig. 2A - Fig. 2A - XRD spectra of kaolinite samples at  $<2 \mu\text{m}$  size fraction (left) and full size distribution (right). The XRD spectra of the bulk samples are labelled to indicate the identified minerals (K: kaolinite; Q: quartz; I: illite/mica; C: calcite and D: dolomite). The same pattern exist in the  $<2 \mu\text{m}$  size fraction data.

Fig. 2B –  $2\theta$  scan of kaolinite showing the kaolinite peaks and background intensity positions used in the calculation of the Hinckley index for Snobrite

Fig. 3 - SEM images show relatively smooth basal surfaces of Snobrite (A), broken edges and ragged shape of Q38 (B) and slightly rounded platelets and micro-islands in KGa2 crystallites (C)

Fig. 4 - Size distribution of different kaolinite samples as estimated by Malvern light scattering

Fig. 5 - A comparison of the zeta potential curves of Snobrite, Q38 and KGa2 in 0.001M KCl solution

Fig. 6 - The potentiometric titration curves of Snobrite, Q38 and KGa2

Fig. 7 - A comparison of the yield stresses of Snobrite, Q38 and KGa2 suspensions

Fig. 8 - A comparison of the shear thinning indices of Snobrite, Q38 and KGa2 suspensions

## FIGURES

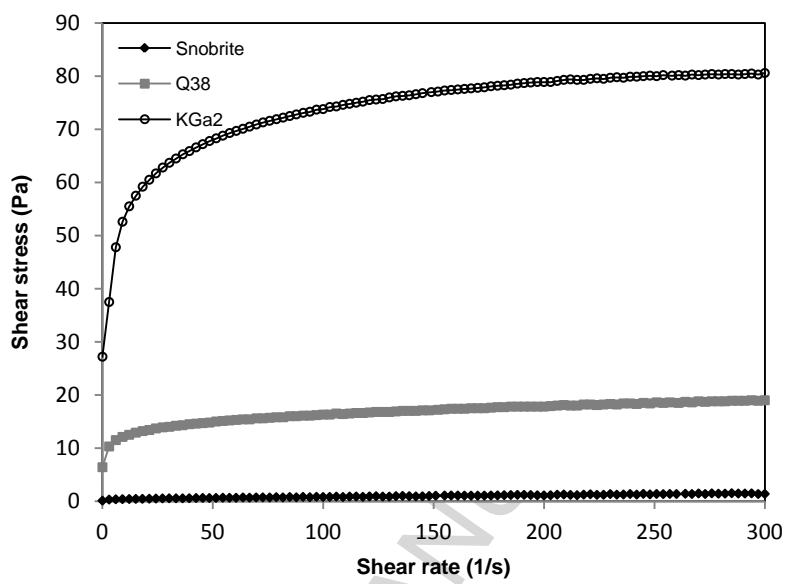
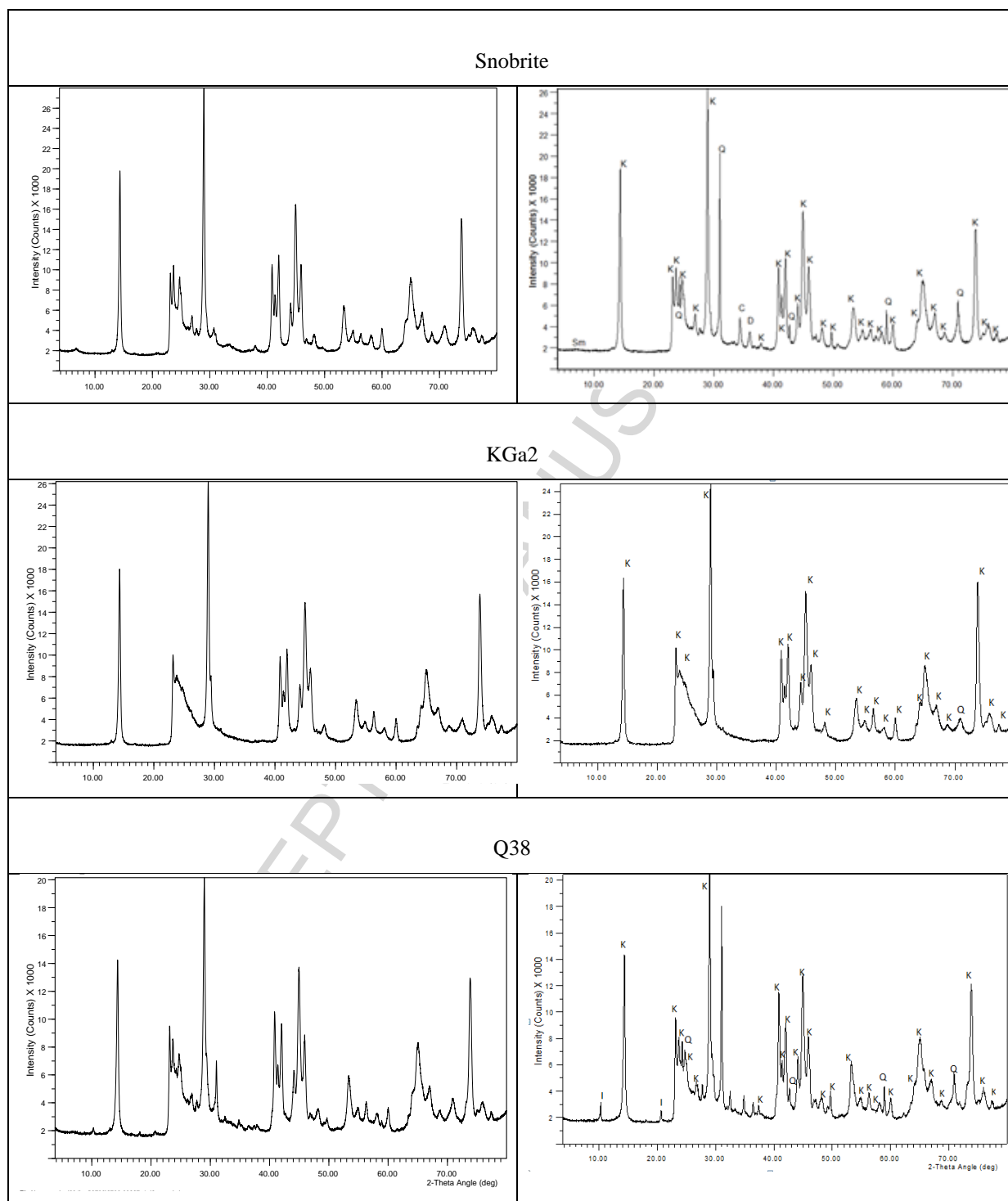


Fig. 1

**Fig. 2A**

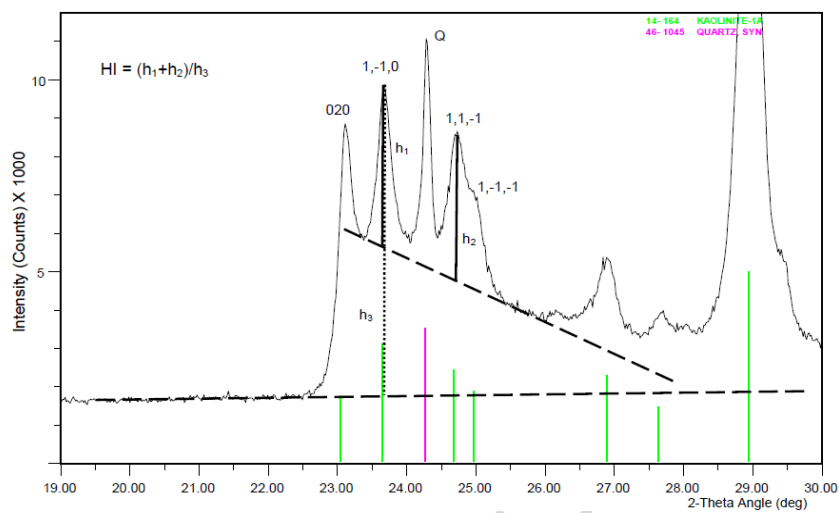


Fig. 2B

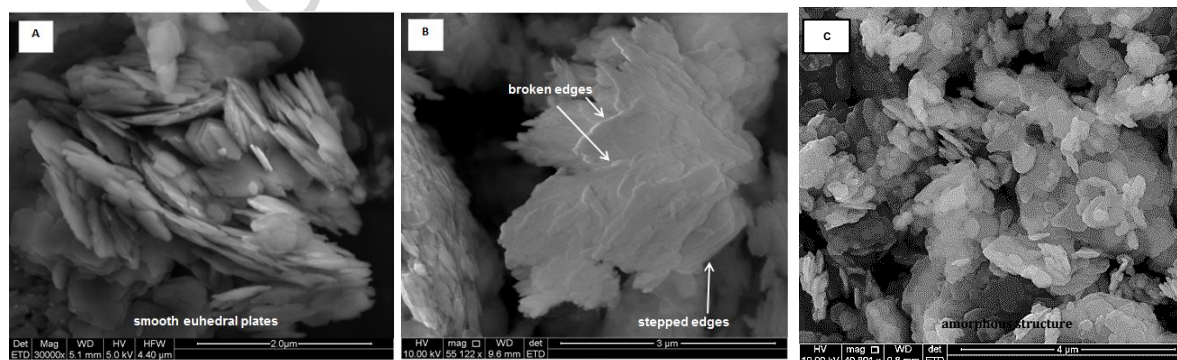


Fig. 3

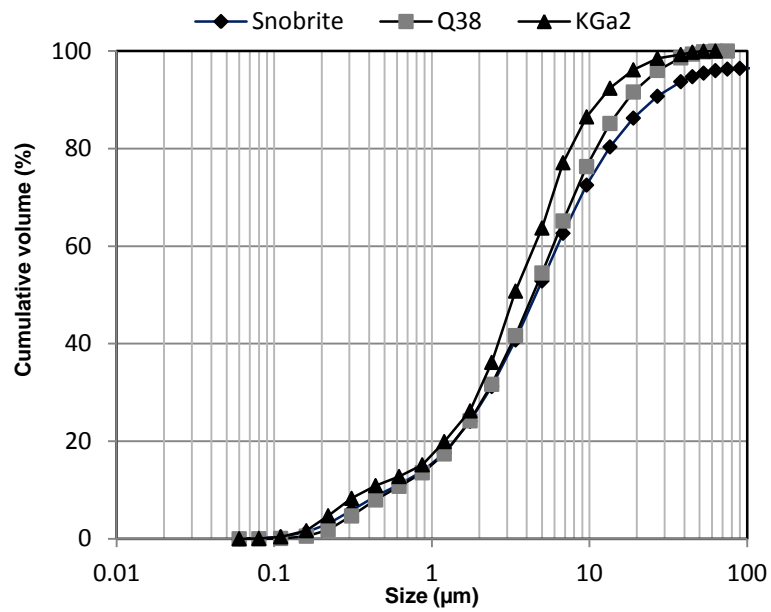


Fig. 4

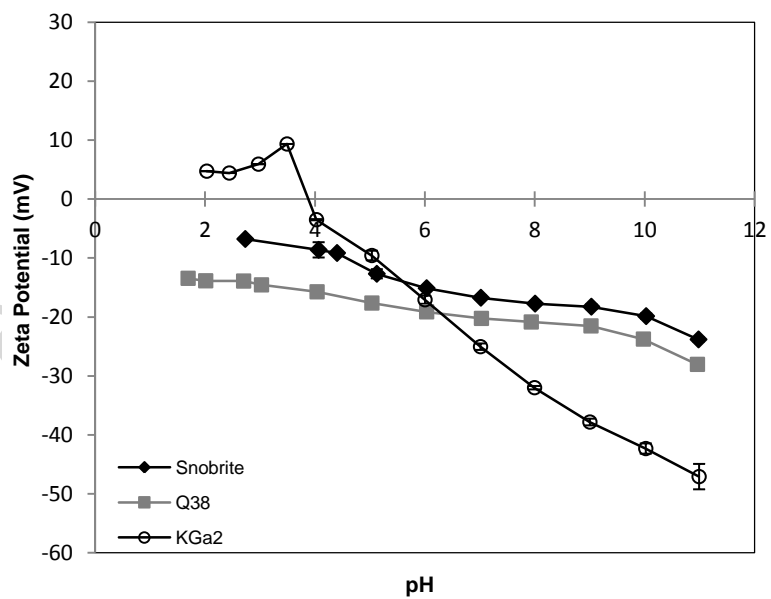


Fig. 5

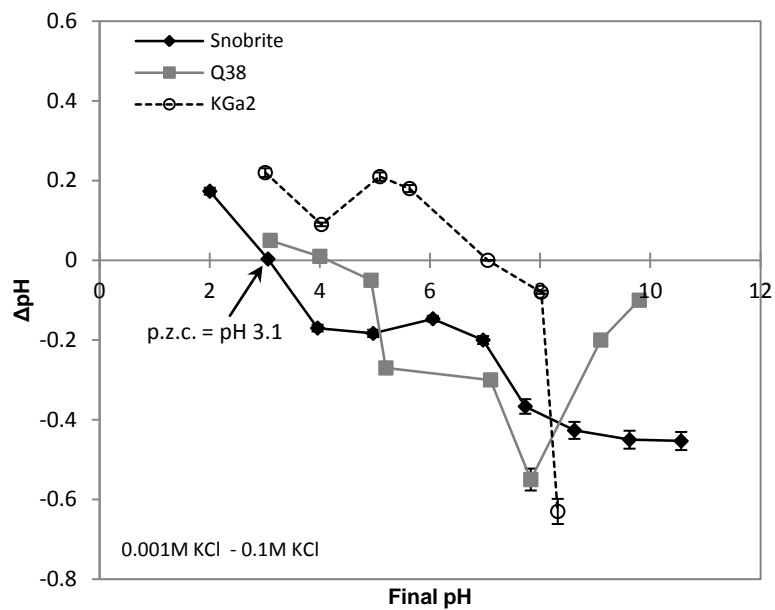


Fig. 6

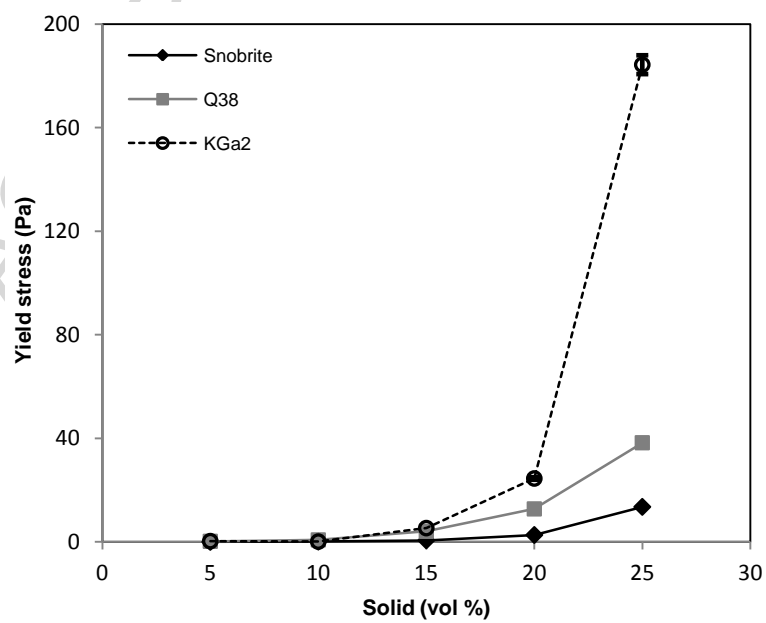


Fig. 7



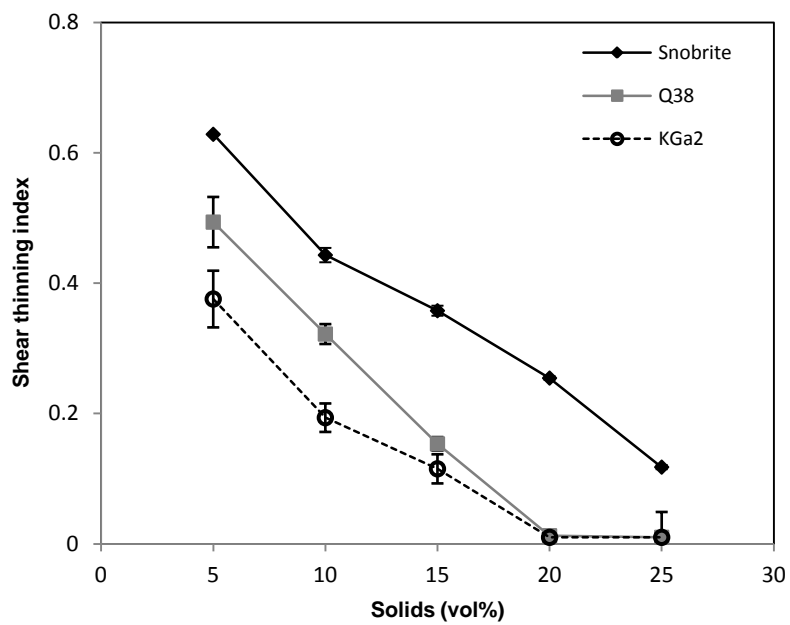
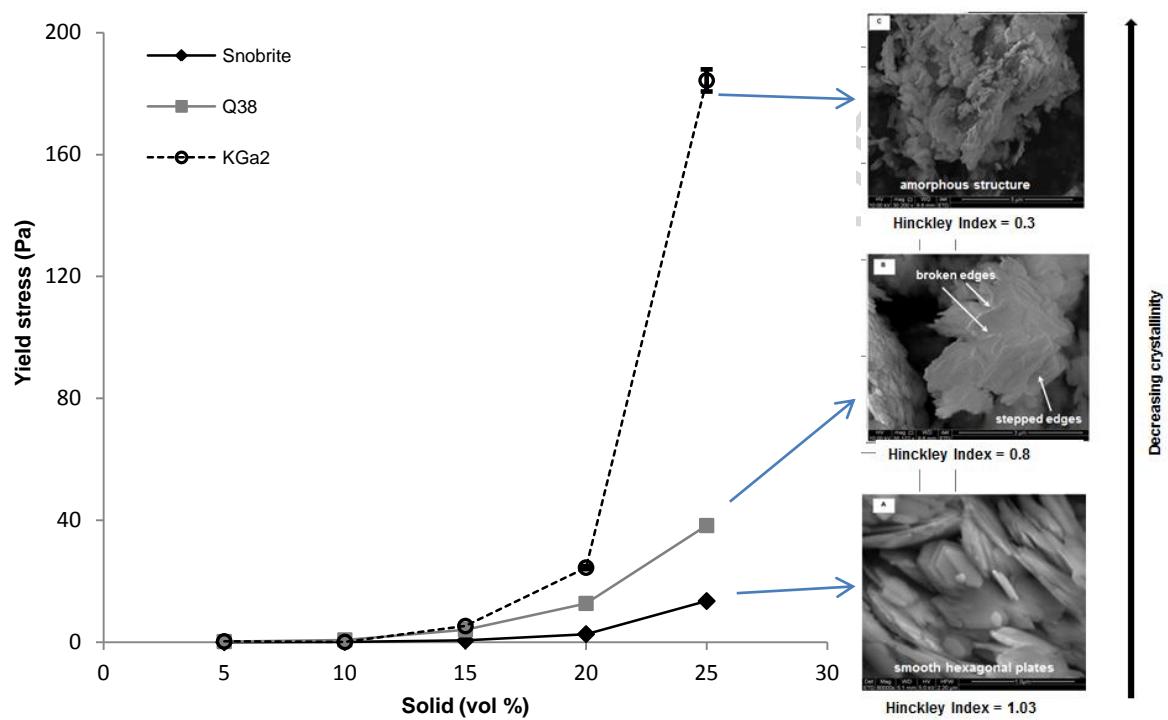


Fig. 8



Graphical abstract

## Highlights

Hinckley index, calculated from XRD spectra estimates the crystallinity of kaolinite

Well crystallised kaolinite has relatively smooth basal planes and a smaller surface area than poorly crystallised kaolinite

Kaolinite samples of different crystallinity present different surface charge properties

The surface charge of well crystallised kaolinite samples represent the charge properties of the extensive smooth basal planes

Low crystallinity kaolinite samples present higher suspension yield stresses and viscosities